

Electronic Supplementary Information

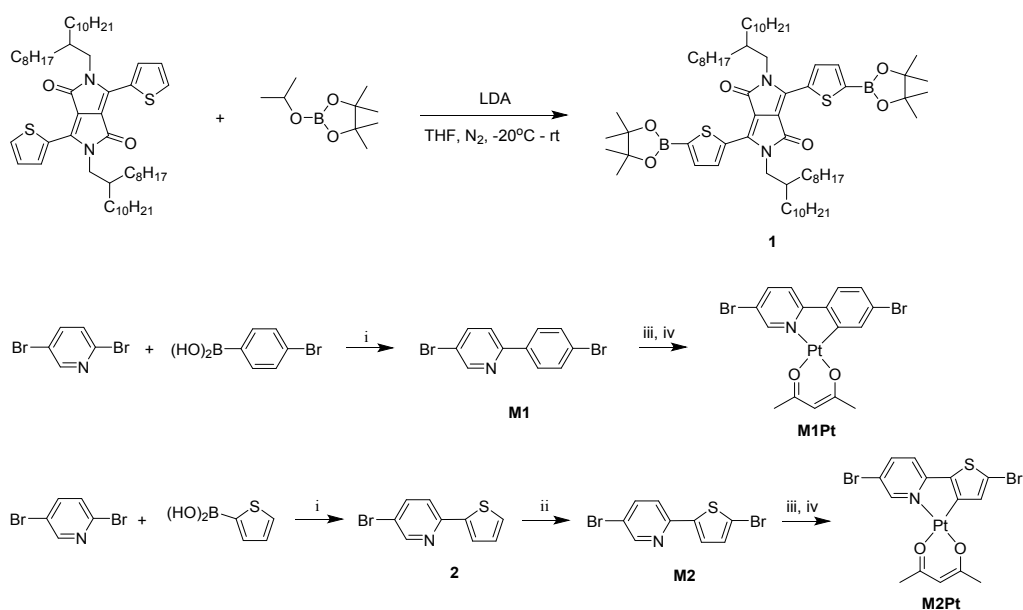
1. General Methods

All chemicals were purchased from Alfa-Aesar, J&K and Sigma-Aldrich, and used without further purification. All solvents were purified and dried following standard procedures^{S1} unless otherwise stated. Flash chromatography was carried out with silica gel (200-300 mesh), and analytical TLC was performed with silica gel GF254 plates. Fourier transform infrared (FTIR) spectra were recorded on an Excalibur HE 3100 (Varian, USA) through the KBr pellet technique in wavenumber region from 4000 cm⁻¹ to 400 cm⁻¹. ¹H NMR and ¹³C NMR spectra were measured on a Bruker AVANCE III 400 and 500 MHz spectrometers. Elemental analysis was performed on a Carlo Erba model 1160 elemental analyzer. Gel permeation chromatography (GPC) analysis was performed on an PL-GPC 220 high temperature chromatograph at 150 °C equipped with an IR5 detector; polystyrene was used as the calibration standard and 1,2,4-trichlorobenzene as eluent; the flow rate was 1.0 mL/min. Ultraviolet-visible-near infrared (UV-vis-NIR) transmission spectra were obtained using Cary 5000 (Varian, USA) spectrophotometer. Thermal gravimetric analysis (TGA) measurements were carried out on a SHIMADZU DTG-60 instruments under a dry nitrogen flow, heating from room temperature to 550 °C, with a heating rate of 10 °C/min. The nonlinear optical properties of the copolymers were investigated by the open/close-aperture Z-scan technology with a Q-switched Nd:YAG pulse laser under the wavelengths of 532 nm and 1064 nm.

2. Synthetic and characterizations

Copolymers were synthesized through Suzuki cross-coupling reaction between polymeric monomers of DPP-based borate (**1**) and corresponding bromide monomers (**M1**, **M2** and **M1Pt**, **M2Pt**). Monomers **1**, **M1**, **M2**, and corresponding Pt(II)-incorporated monomers **M1Pt** and **M2Pt** were prepared with modified methods according to the previous reports.^{S2}

a) the synthetic procedures of monomers.

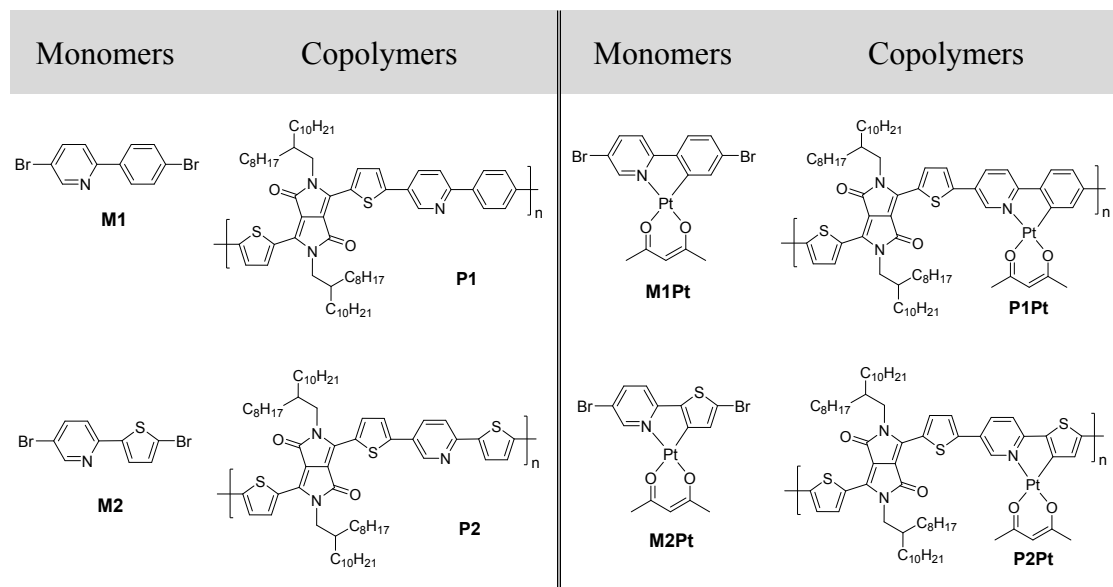
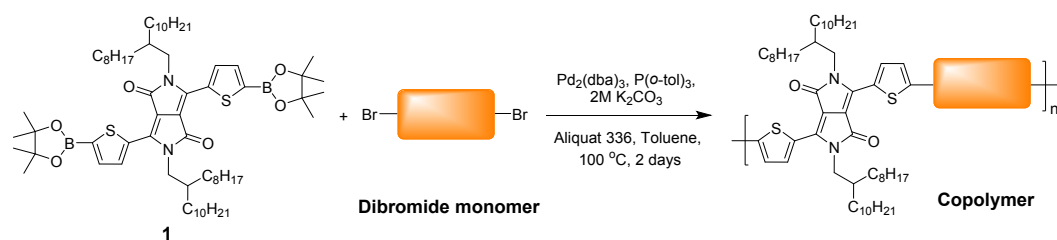


Conditions:

i: K₂CO₃, Pd(PPh₃)₄, THF, H₂O, 60 °C, 24h; ii: NBS, CHCl₃, r.t., overnight;

iii: K₂PtCl₄, H₂O, 2-ethoxyethanol, 80 °C, 24h; iv: Na₂CO₃, 2,4-pentanedione, 2-ethoxyethanol, 100 °C, 24h.

b) the synthetic procedures of copolymers.



The general synthetic procedures of copolymers: Monomers compound **1** (1.0 equiv.), corresponding dibromide compounds (1.0 equiv.), tri(*o*-tolyl)phosphine [P(*o*-tol)₃] (0.16 equiv.) and a catalytic amount of Aliquat 336 were placed in a Schlenk tube. Then toluene (10mL) and aqueous K₂CO₃ (2.0 M, 2.0 mL) was added. Finally, the catalyst tris(dibenzyl-ideneacetone)-dipalladium (0) Pd₂(dba)₃ (0.02 equiv.) was added. The tube was charged with nitrogen under a freeze–pump–thaw cycle for three times. The mixture was stirred at 100 °C for 48 h under nitrogen and then cooled to room temperature. The resulting mixture was poured into methanol. Dark precipitates were filtered off and subjected to Soxhlet extraction eluting with methanol, hexane, acetone, and chloroform to remove the remaining monomers, oligomers, and catalytic impurities. Copolymer was collected and dried under vacuum at 50 °C for 48 h.

The synthesis of P1. Compound **1** (150.0 mg, 135 μmol), **M1** (42.3 mg, 135 μmol), P(*o*-tol)₃ (6.6 mg, 21.6 μmol), and Pd₂(dba)₃ (2.5 mg, 2.7 μmol) were used. The purified

polymer was collected to give **P1** as a deep blue solid (84.0 mg, yield 61%). ¹H NMR (500 MHz, 1,1,2,2-tetrachloroethane-*d*₂, 373 K): δ = 9.11-8.91 (m, br, 3H), 8.22-7.60 (m, br, 8H), 4.13 (s, br, 4H), 2.08 (s, br, 2H), 1.47-1.32 (m, br, 64H), 0.93 (s, br, 12H). *M_w/M_n* (GPC) = 24.5/16.8 kg mol⁻¹. Elemental analysis calcd (%) for (C₆₅H₉₃N₃O₂S₂)_n: C, 77.10; H, 9.26; N, 4.15; S, 6.33. Found: C, 76.56; H, 9.31; N, 4.12; S, 6.30. IR spectrum (KBr, cm⁻¹): 3082, 2953, 2922, 2852, 1664, 1553, 1468, 1433, 1402, 1379, 1232, 1153, 1109, 1072, 1026, 1010, 890, 734, 717, 633, 503.

The synthesis of P2. Compound **1** (150.0 mg, 135 μmol), **M2** (43.1 mg, 135 μmol), P(*o*-tol)₃ (6.6 mg, 21.6 μmol), and Pd₂(dba)₃ (2.5 mg, 2.7 μmol) were used. The purified polymer was collected to give **P2** as a deep blue solid (99.5 mg, yield 72%). ¹H NMR (500 MHz, 1,1,2,2-tetrachloroethane-*d*₂, 373 K): δ = 8.94-8.70 (m, br, 3H), 7.67-7.18 (m, br, 6H), 4.06 (m, br, 4H), 2.05 (m, br, 2H), 1.51-1.32 (m, br, 64H), 0.91 (m, br, 12H). *M_w/M_n* (GPC) = 66.8/35.6 kg mol⁻¹. Elemental analysis calcd (%) for (C₆₃H₉₁N₃O₂S₃)_n: C, 74.29; H, 9.01; N, 4.13; S, 9.44. Found: C, 73.81; H, 9.12; N, 4.10; S, 9.41. IR spectrum (KBr, cm⁻¹): 3069, 2955, 2923, 2951, 1668, 1556, 1472, 1428, 1402, 1380, 1230, 1104, 1065, 809, 791, 731, 713, 635.

The synthesis of P1Pt. Compound **1** (100.0 mg, 90 μmol), **M1Pt** (55.0 mg, 90 μmol), P(*o*-tol)₃ (5.0 mg, 12 μmol), and Pd₂(dba)₃ (3.0 mg, 2.7 μmol). Copolymer **P1Pt** was collected as a dark blue solid (103.0 mg, yield 88%). *M_w/M_n* (GPC) = 19.8/9.4 kg mol⁻¹. Elemental analysis calcd (%) for (C₇₀H₉₉N₃O₄PtS₂)_n: C, 64.39; H, 7.64; N, 3.22; S, 4.91. Found: C, 65.56; H, 7.41; N, 3.12; S, 4.80. IR spectrum (KBr, cm⁻¹): 3050, 2937, 2847, 2360, 2342, 1664, 1575, 1515, 1462, 1396, 1325, 1265, 1223, 1098, 809.

The synthesis of P2Pt. Compound **1** (223.0 mg, 200 μmol), **MPt2** (121.0 mg, 200 μmol), P(*o*-tol)₃ (12.2 mg, 40 μmol), and Pd₂(dba)₃ (9.2 mg, 10 μmol). Copolymer **P2Pt** was collected as a dark blue solid (226.0 mg, yield 87%). *M_w/M_n* (GPC) = 82.0/16.4 kg mol⁻¹. Elemental analysis calcd (%) for (C₆₈H₉₇N₃O₄PtS₃)_n: C, 62.26; H, 7.45; N, 3.20; S, 7.33. Found: C, 60.54; H, 7.19; N, 3.36; S, 7.30. IR spectrum (KBr, cm⁻¹): 3058, 2916, 2847, 2352, 1658, 1554, 1467, 1405, 1225, 1070, 1032, 810, 723, 624.

4. TGA of copolymers

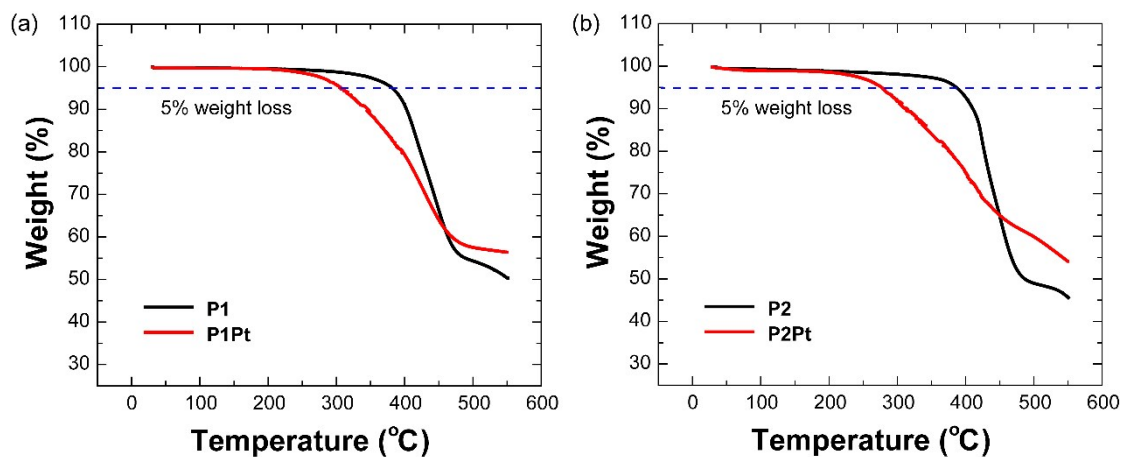


Figure S1. TGA comparison curves of copolymer and corresponding Pt(II)-incorporated copolymers. (a) **P1** ($T_d = 381$ °C) and **P1Pt** ($T_d = 305$ °C); (b) **P2** ($T_d = 387$ °C) and **P2Pt** ($T_d = 276$ °C). Heating rate: 10 °C min^{-1} ; from 25 °C to 550 °C under nitrogen atmosphere. T_d is the decomposition temperature (dash line) at 5% weight loss.

5. Theoretical calculations

All the computational works were performed using Gaussian 16 suite of programs.^{S3} Geometry optimizations and molecular orbital energies calculation were carried out at B3LYP^{S4} correlation function and 6-31G (d,p) level. The fragment contributions^{S5} to molecular orbitals were calculated using Multiwfn software^{S6}. The optimized structures were displayed using Gaussview 5.0^{S7}.

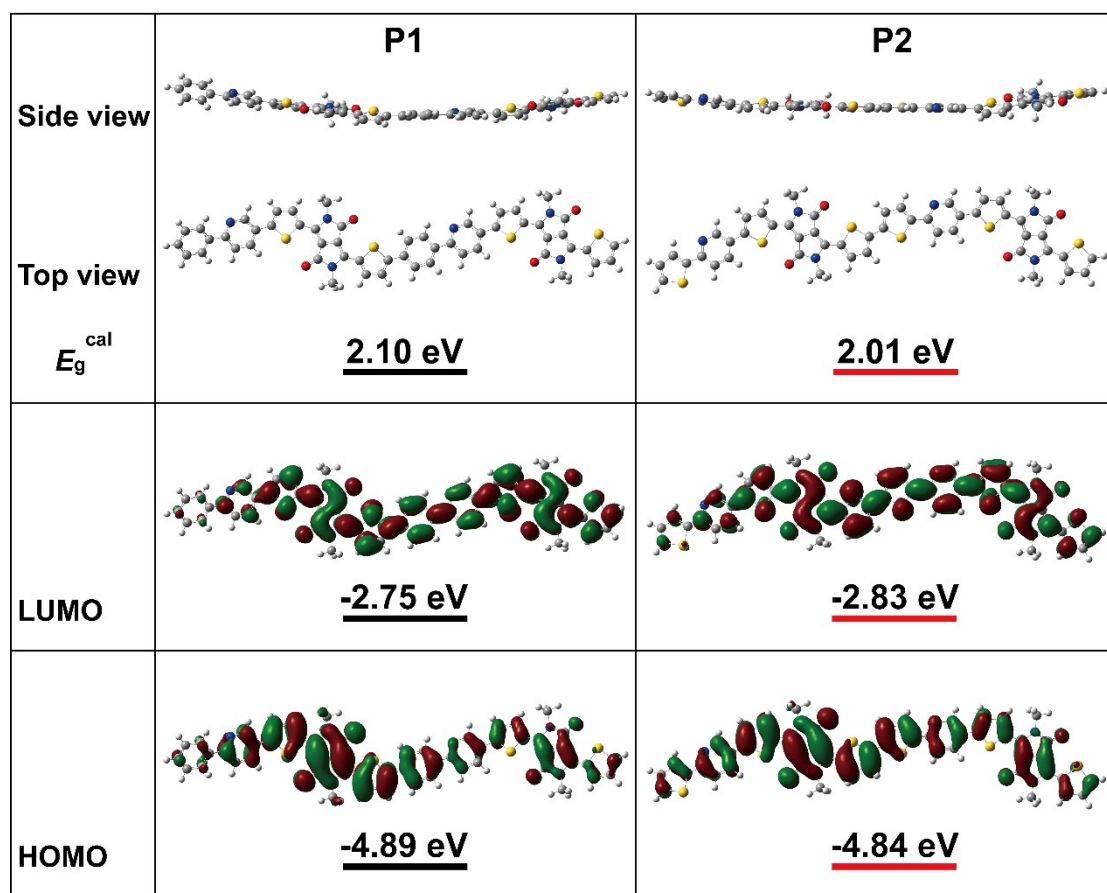


Figure S2. The calculated molecular structures (side and top views), frontier molecular orbits, and HOMO/LUMO energy levels of the repeated two units of copolymers **P1** and **P2**. The alkyl side chain was replaced with methyl group for simplifying computations.

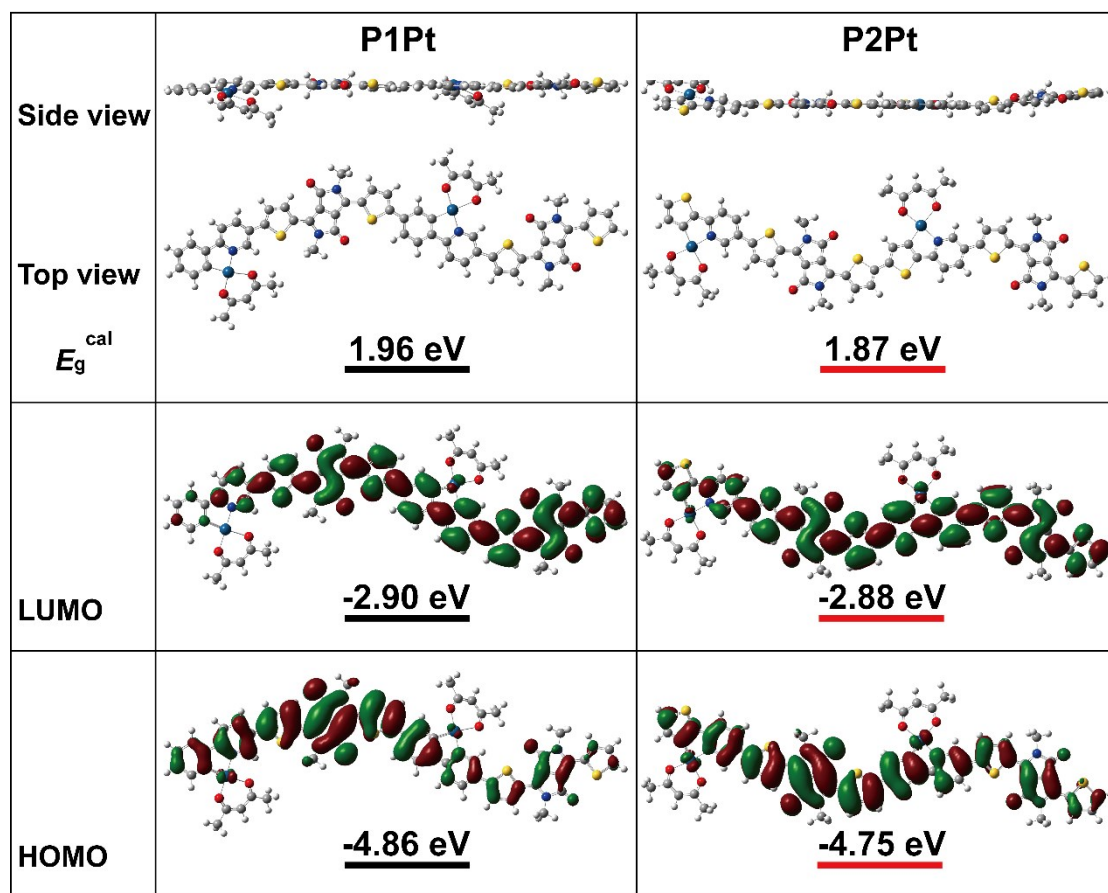
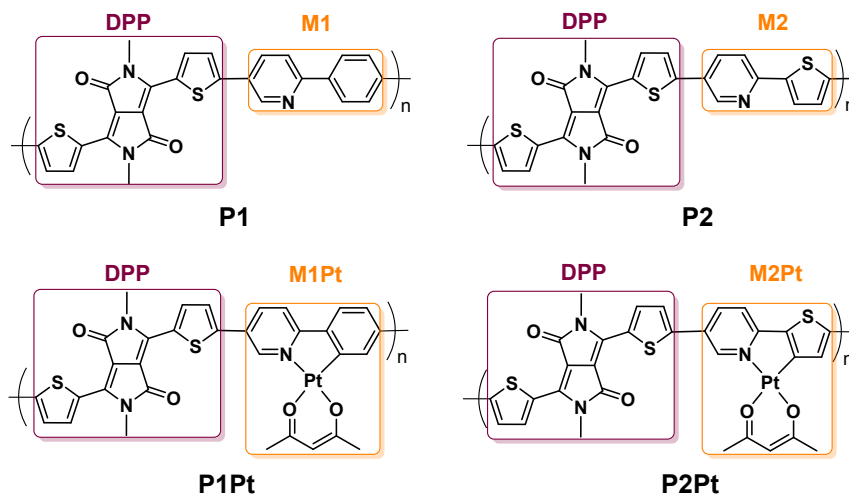


Figure S3. The calculated molecular structures (side and top views), frontier molecular orbits, and HOMO/LUMO energy levels of the repeated two units of copolymers **P1Pt** and **P2Pt**. The alkyl side chain was replaced with methyl group for simplifying computations.

Table S1 The calculated contribution percentage of two conjugated components to LUMO+1, LUMO, HOMO, HOMO-1 of corresponding copolymers.



Copolymers	Components	HOMO-1	HOMO	LUMO	LUMO+1
P1	DPP	94%	86%	80%	90%
	M1	6%	14%	20%	10%
P2	DPP	93%	81%	76 %	89%
	M2	7%	19%	24%	11%
P1Pt	DPP	93%	84%	78%	87%
	M1Pt	7%	16 %	23%	13%
P2Pt	DPP	89%	73%	75%	88%
	M2Pt	11%	27%	25%	12%

6. Z-scan experiments

The detailed description of Z-scan technology: The Z-scan method was introduced in 1989 by Sheik-Bahae *et al.*^{S8} using to determine third-order nonlinear optical (NLO) response. In this work, the nanosecond NLO properties are collected using open-aperture Z-scan technology with a FWHM of 8 ns and a repetition frequency of 10 Hz laser pulse from a Nd:YAG laser under wavelengths of 532 and 1064 nm. The radius of beam waist is 13.5 and 27 μm for 532 and 1064 nm laser pulses, respectively. The picosecond NLO performances are obtained using Z-scan technology with a FWHM of 25 ps and a repetition frequency of 1 KHz laser pulse from a Nd:YAG laser under wavelengths of 532 and 1064 nm. The radius of beam waist is 22.5 and 45 μm for 532 and 1064 nm laser pulses, respectively. The spatial and temporal profiles of the pulse laser presented an approximately Gaussian distribution.

The samples were placed in quartz cuvette with thickness of 1 mm with identical linear transmittance of 70% at 532 nm and fixed on a stepper motor which was controlled by a computer to move along the Z axis reference to the focal point. In the open-aperture measurement, normalized transmittance of 1.0 indicates that the material exhibits no NLO behavior. When the sample exhibits saturable absorption, normalized transmittance above 1.0 will be observed. In contrast, the normalized transmittance below 1.0 indicates that the sample exhibits reverse saturable absorption. In the close-aperture measurement, the nonlinear refractive medium acts as either a negative lens or a positive lens, depending on the sign of the nonlinear refractive index change, and shows self-limiting action via self-focusing or self-defocusing of the beam translating through it. The normalized transmittance appear peak and valley successively when samples move from -Z to +Z indicating self-focusing, in contrast, the normalized transmittance appear valley and peak successively when samples move from -Z to +Z indicating self-defocusing.

The open-aperture Z-scan equipment was used for optical limiting experiment. The samples were placed in quartz cuvette with thickness of 1 mm and identical linear

transmittance of 70% at 532 nm and fixed on the stepper motor which has been moved to the laser focus point.

The nonlinear fitting of Z-scan curves: The open-aperture Z-scan curves can be fitted into transmittance equation for a third-order nonlinear process:^{S9}

$$T = 1 - \beta I_0 L_{eff} / [\sqrt{8}(1 + z/z_0)^2]$$

Where T is the normalized transmittance, β is the effective nonlinear extinction coefficient, I_0 is the input intensity at the focus, and z is the sample position. The effective thickness L_{eff} of the sample is given by $L_{eff} = [1 - \exp(-\alpha_0 l)] / \alpha_0$ (where l is the sample thickness), $\alpha_0 = (-\ln T_0) / l$, α_0 is the linear absorption coefficient at a given wavelength, T_0 is the linear transmittance. $z_0 = kw_0^2 / 2$, z_0 is the Rayleigh diffraction length. w_0 is the beam waist at focal point $z = 0$. $k = 2\pi / \lambda$, where k is the wave vector and λ is the laser wavelength.

The close-aperture Z-scan curves are fitted into transmittance by using following equation:^{S9, S10}

$$T = 1 - \frac{4\Delta\Phi_0 z}{\left[\left(\frac{z}{z_0}\right)^2 + 9\right]\left[\left(\frac{z}{z_0}\right)^2 + 1\right]}$$

By using variable transmittance values of the closed-aperture Z-scan, the nonlinear phase shift $\Delta\Phi_0$ and the nonlinear refractive n_2 were determined as following:

$$\Delta\Phi_0 = \frac{\Delta T_{P-V}}{0.466(1-S)^{0.25}}$$

Where $\Delta T = T_P - T_V$; T_P and T_V are the normalized peak and valley transmittances. S was defined as the ratio of the light passing through the aperture to the light in front the aperture.

The n_2 values can be calculated by using equation:

$$n_2 = \frac{\lambda \Delta \Phi_0}{6.28 I_0 L_{eff}}$$

The imaginary parts of the third order nonlinear optical susceptibility $\chi^{(3)}$ are determined from the following equation:

$$Im \chi^{(3)} = \frac{n_0^2 \epsilon_0 c \lambda \beta}{2\pi}$$

where n_0 is the linear refractive index, ϵ_0 is the permittivity of free space, c is the speed of light, λ is the laser wavelength and β is the effective nonlinear extinction coefficient.

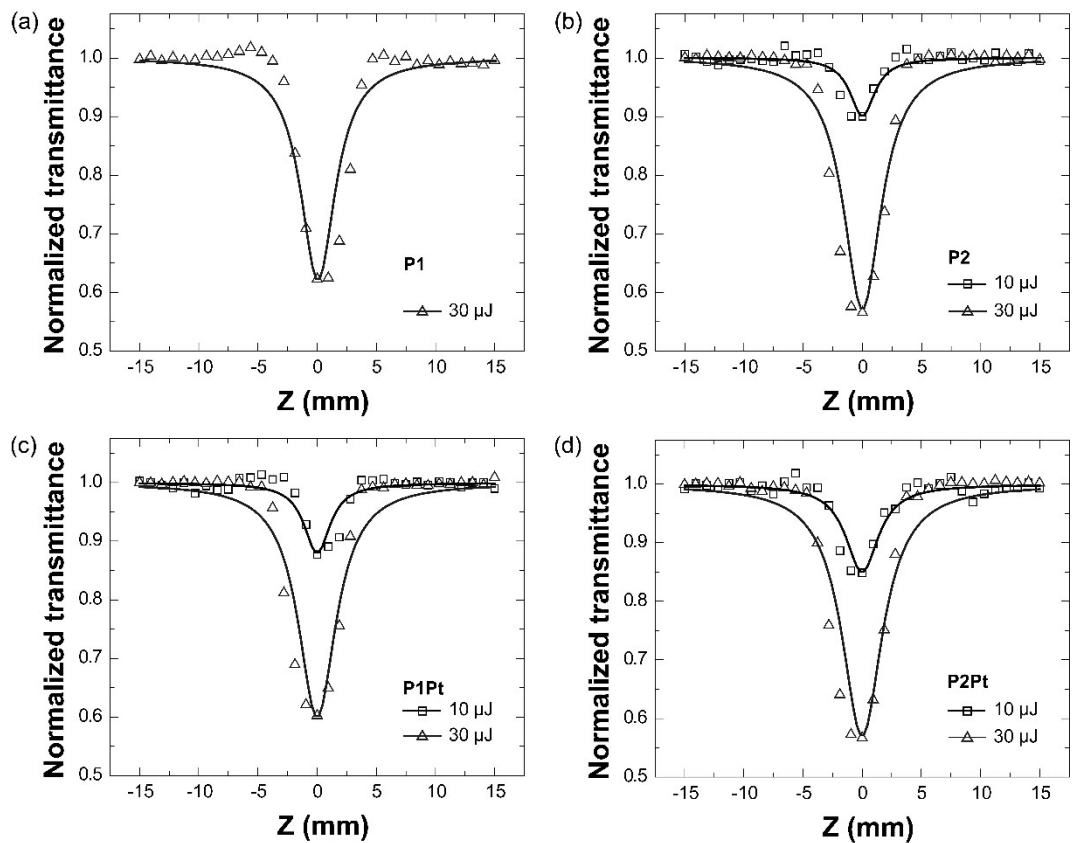


Figure S4. The NLO properties of copolymers (a) **P1**, (b) **P2** and (c) **P1Pt**, (d) **P2Pt** responding to 10 and 30 μJ ns laser pulse under 532 nm.

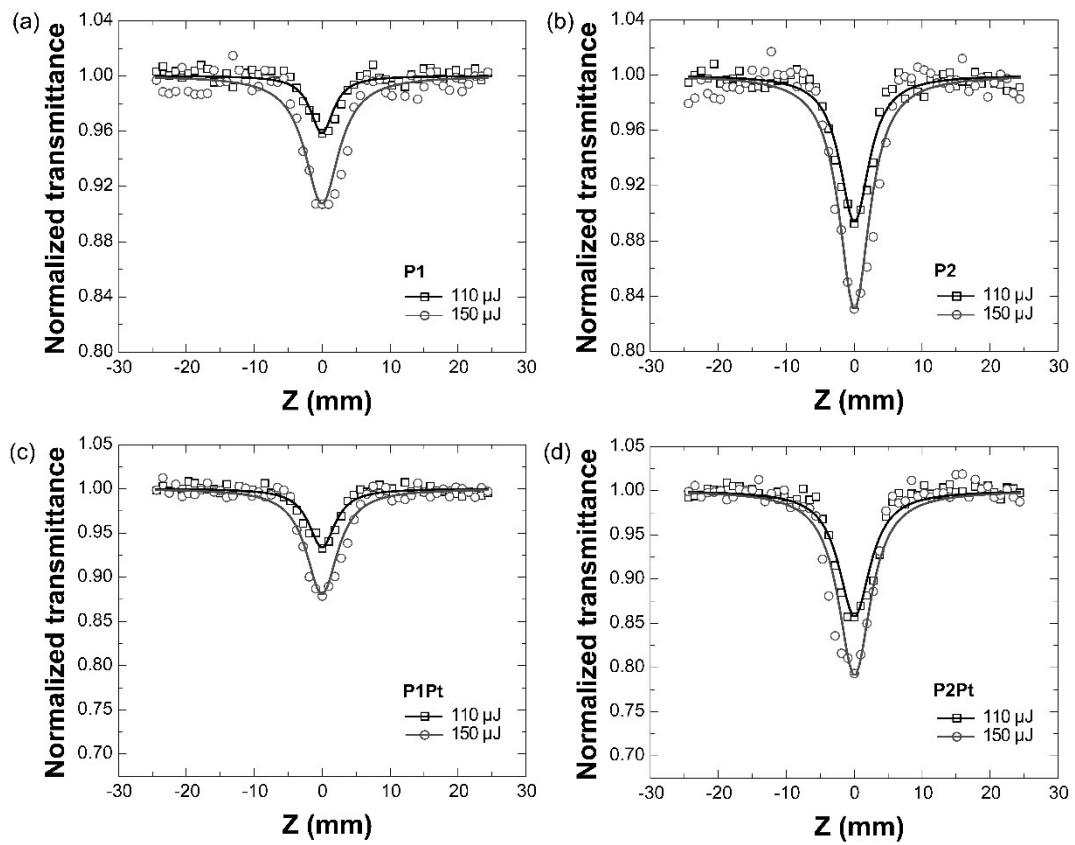


Figure S5. The NLO properties of copolymers (a) **P1**, (b) **P2** and (c) **P1Pt**, (d) **P2Pt** responding to 110 and 150 μJ ns laser pulse under 1064 nm.

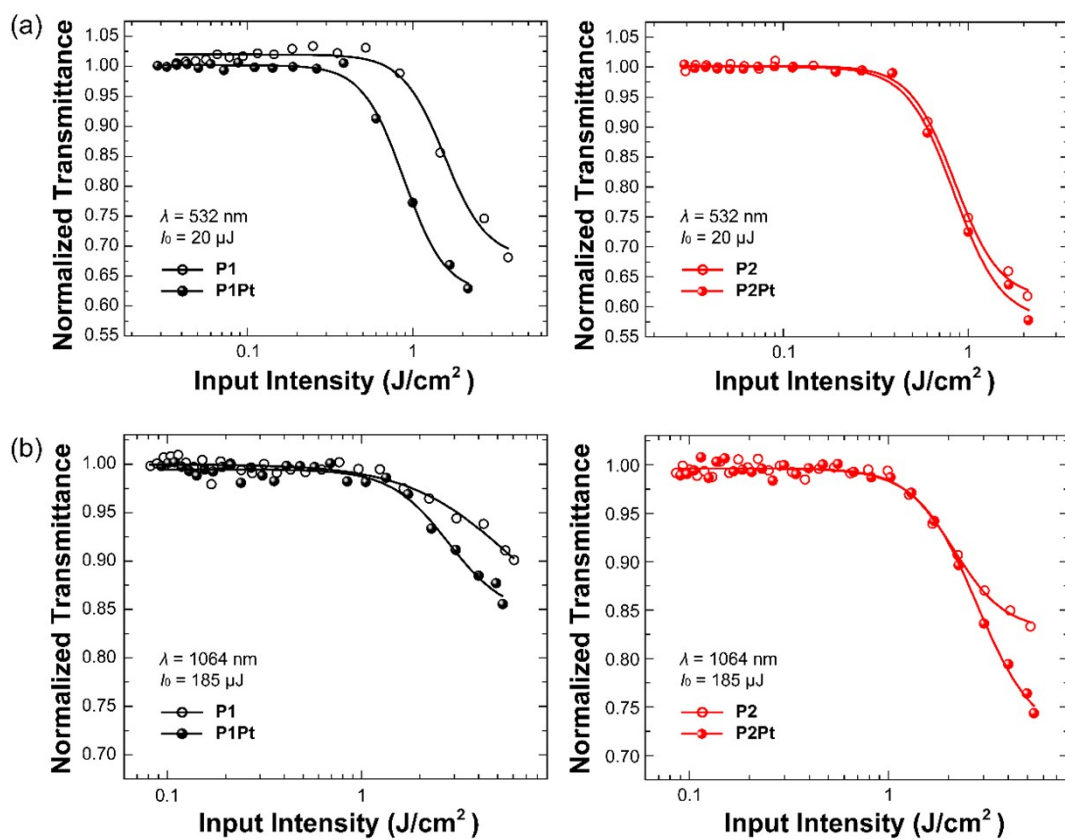


Figure S6. Normalized transmittance vs. Input intensity plots extracting through nonlinear fitting from Z-scan curves upon the excitation of (a) 20 μJ nanosecond laser pulse under 532 nm and (b) 185 μJ nanosecond laser pulse under 1064 nm.

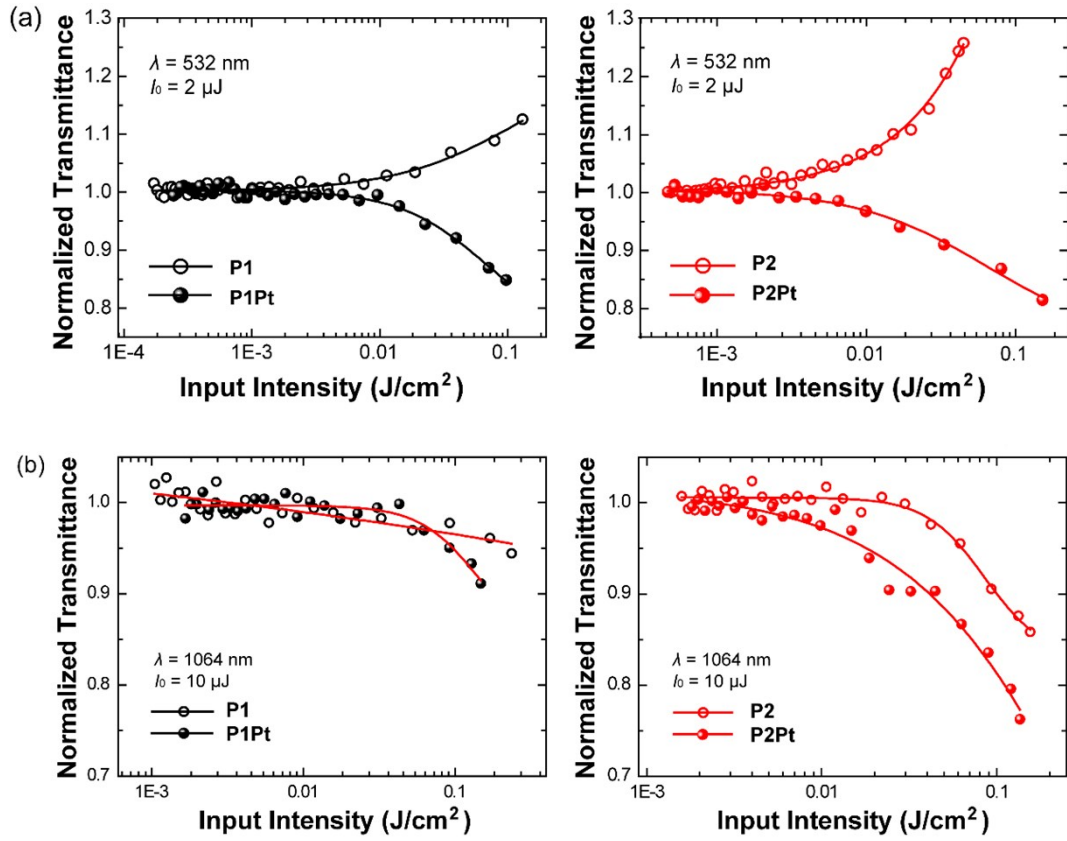


Figure S7. Normalized transmittance vs. Input intensity plots extracting through nonlinear fitting from Z-scan curves upon the excitation of (a) 2 μJ picosecond laser pulse under 532 nm and (b) 10 μJ picosecond laser pulse under 1064 nm.

3. The high temperature ^1H NMR, GPC traces, and FTIR spectra of copolymers.

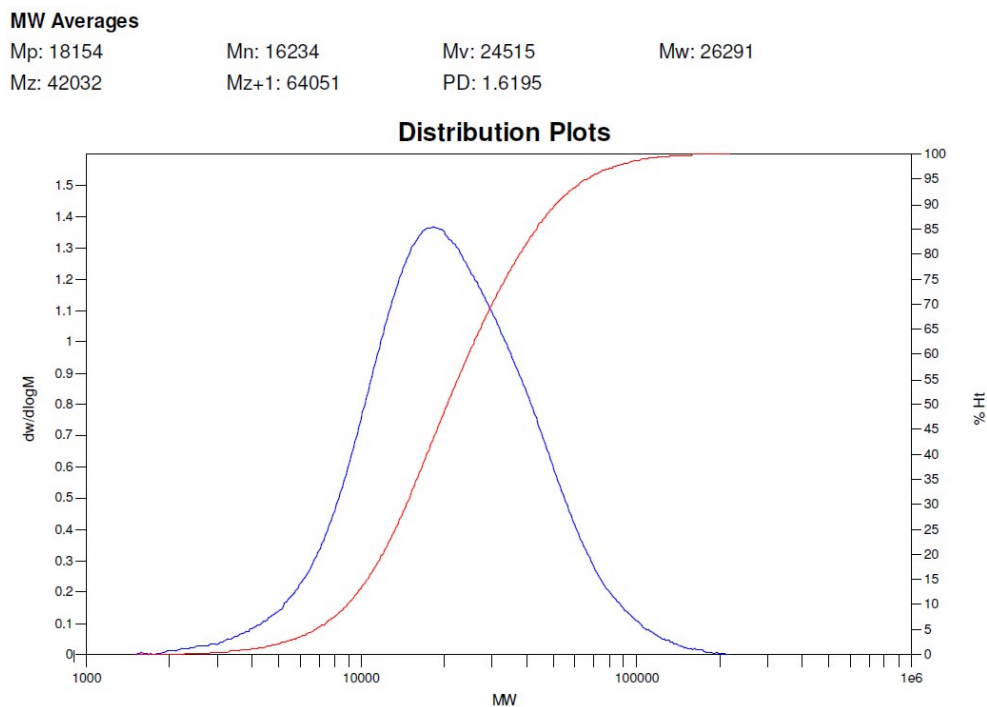


Figure S8. The GPC trace for copolymer **P1**.

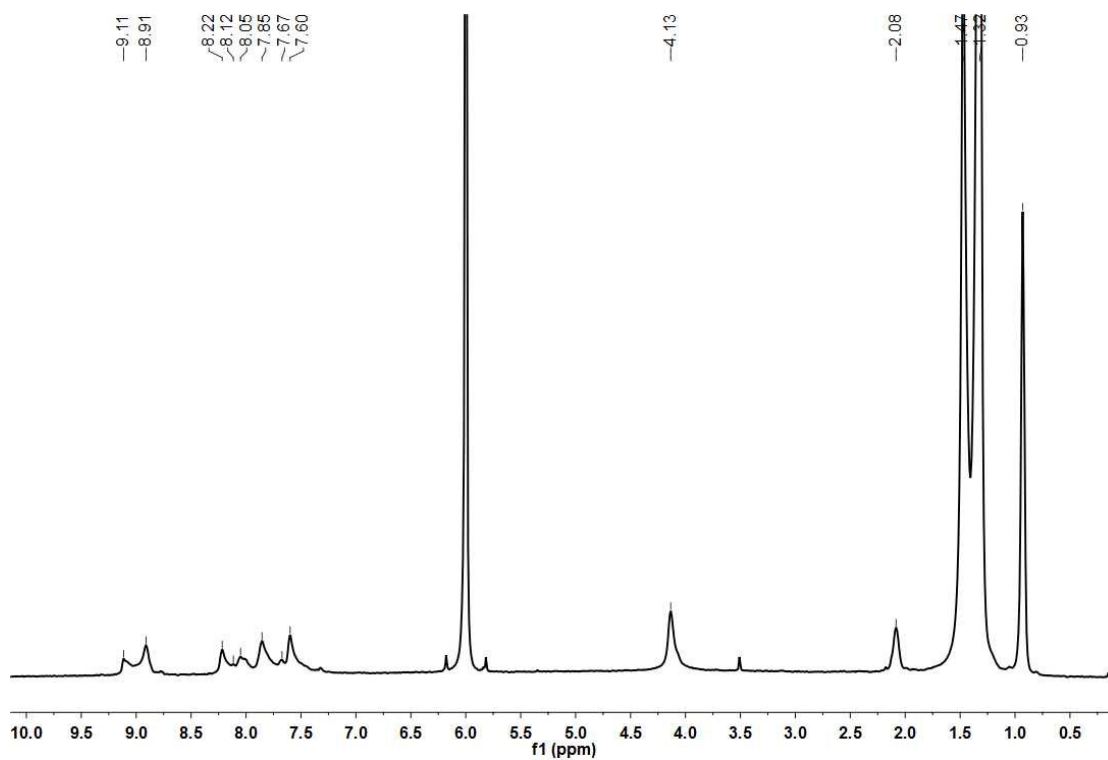


Figure S9. The ^1H NMR spectrum of copolymer **P1**.

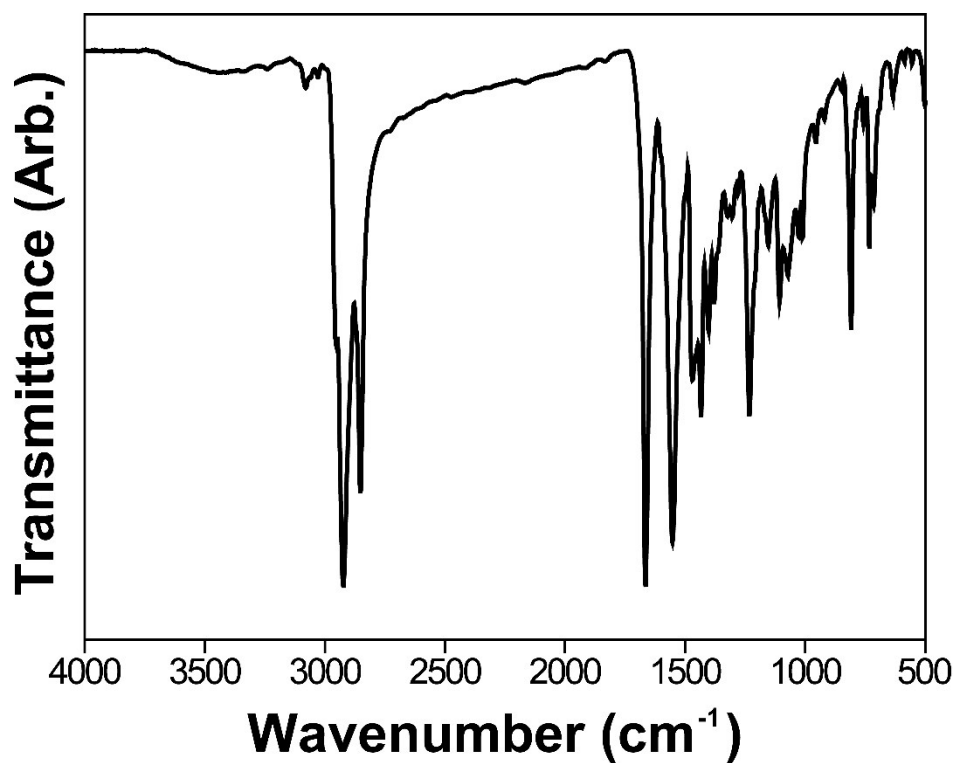


Figure S10. The FTIR spectrum of copolymer **P1**.

MW Averages

Mp: 54965	Mn: 35553	Mv: 66810	Mw: 73604
Mz: 133871	Mz+1: 210753	PD: 2.0703	

Distribution Plots

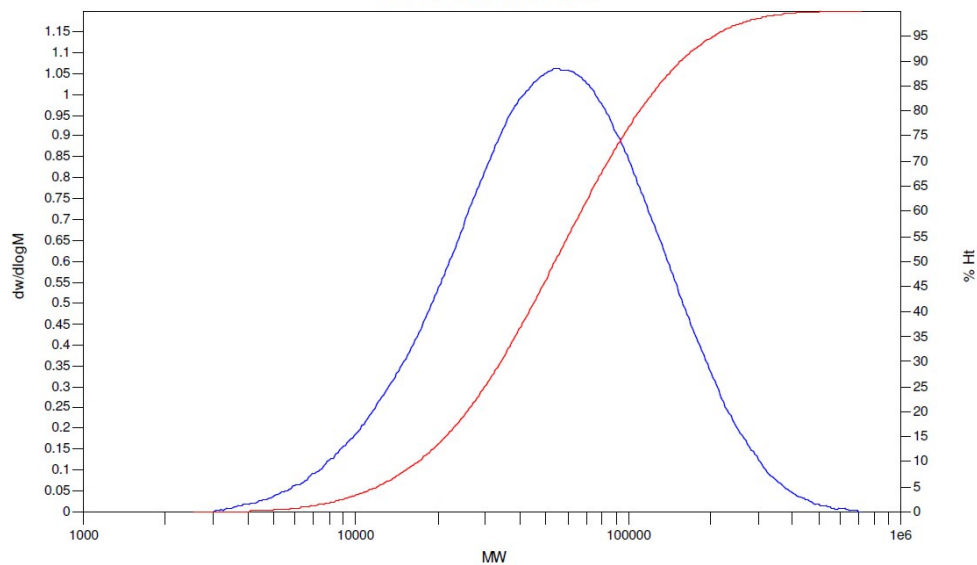


Figure S11. The GPC trace for copolymer **P2**.

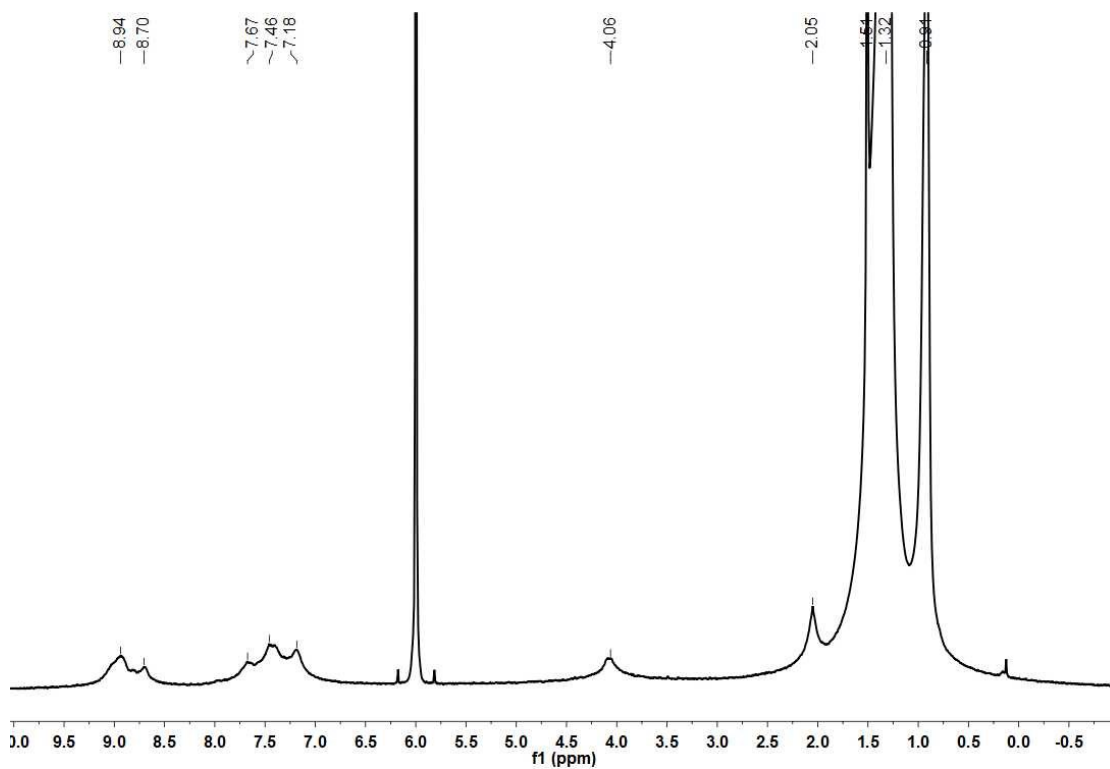


Figure S12. The ^1H NMR spectrum of copolymer **P2**.

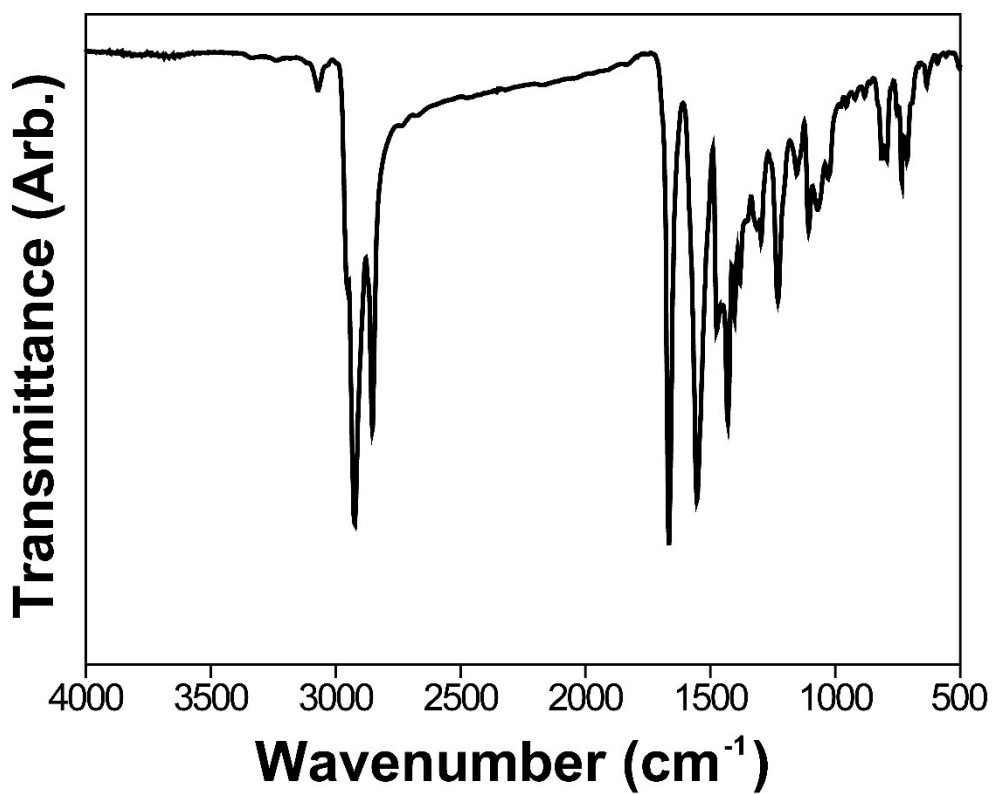


Figure S13. The FTIR spectrum of copolymer **P2**.

MW Averages

Mp: 16393

Mn: 9396

Mv: 17982

Mw: 19832

Mz: 35327

Mz+1: 52073

PD: 2.1107

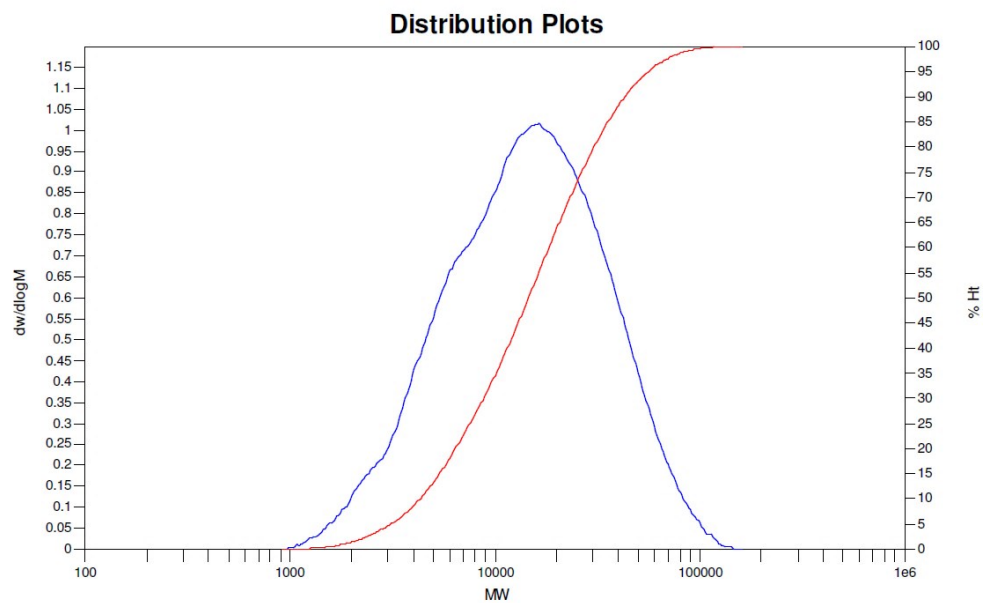


Figure S14. The GPC trace for copolymer **P1Pt**.

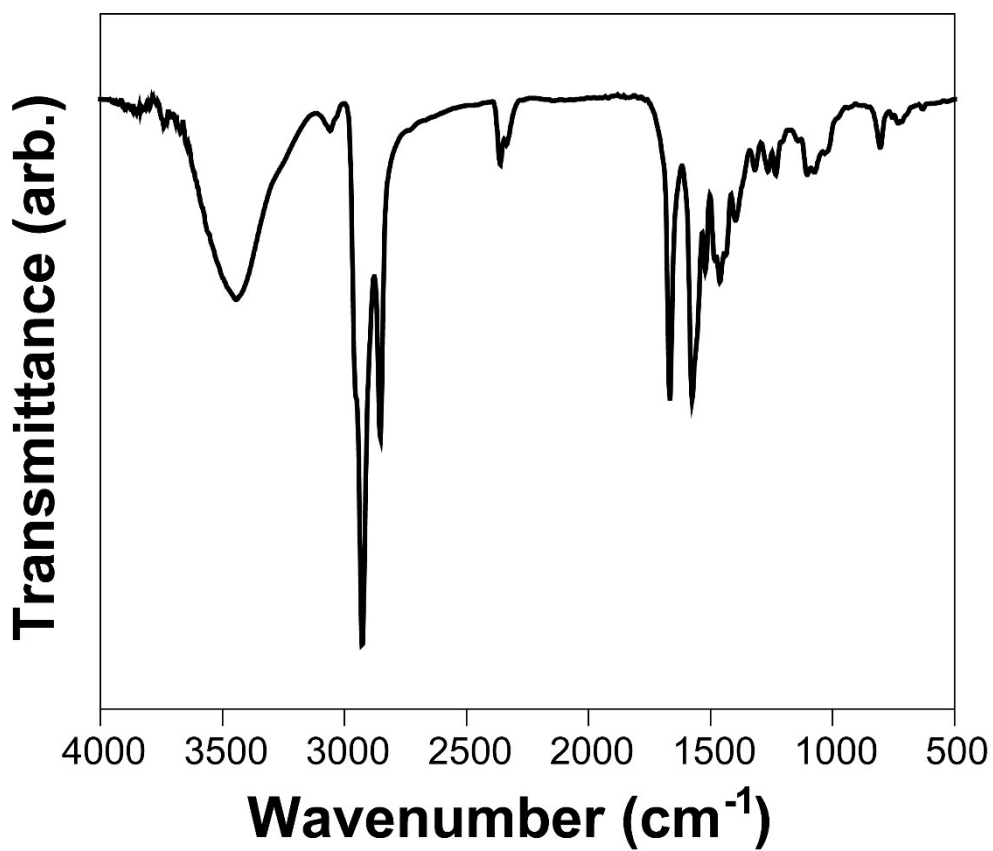


Figure S15. The FTIR spectrum of copolymer **P1Pt**.

MW Averages

Mp: 34938

Mn: 16391

Mv: 61104

Mw: 82024

Mz: 605514

Mz+1: 1669224

PD: 5.0042

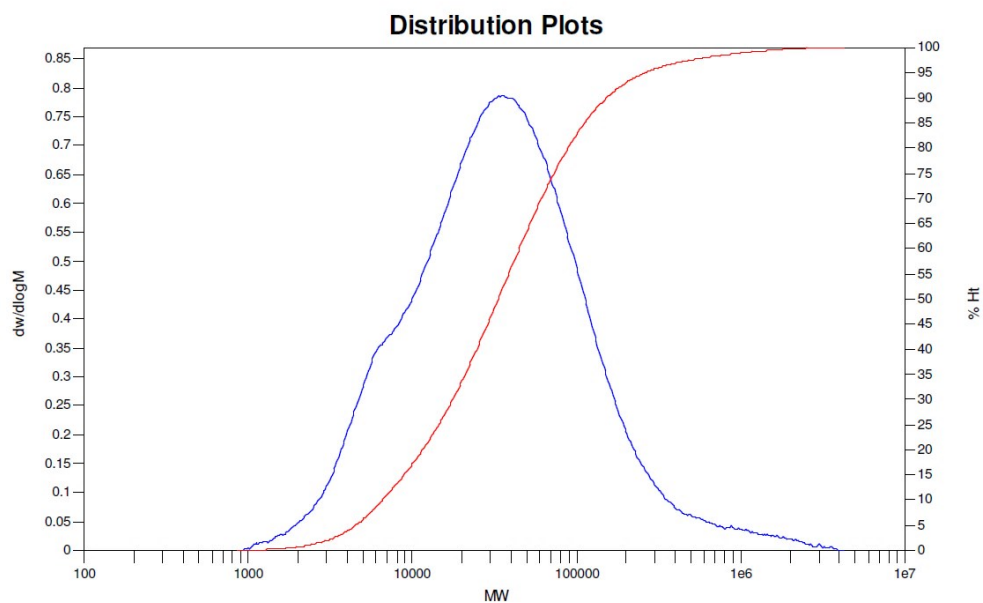


Figure S16. The GPC trace for copolymer **P2Pt**.

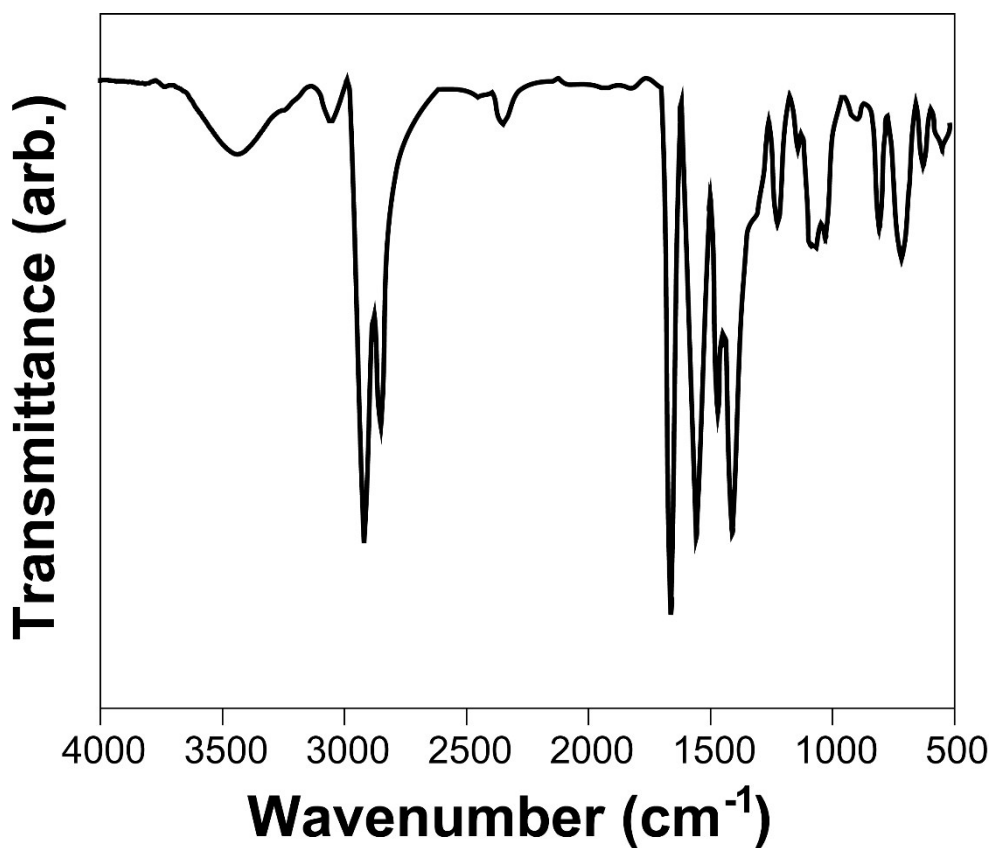


Figure S17. The FTIR spectrum of copolymer **P2Pt**.

6. References

- S1. Purification of Laboratory Chemicals, 5th ed., Wilfres L.F. Armarege, Christina L.L.Chai.
- S2. a) H. Burckstummer, A. Weissenstein, D. Bialas and F. Wurthner, *J. Org. Chem.*, **2011**, *76*, 2426–2432; b) H.-F. Huang, S.-H. Xu, Y.-B. He, C.-C. Zhu, H.-L. Fan, X.-H. Zhou, X.-C. Gao and Y.-F. Dai, *Dyes Pigm.*, **2013**, *96*, 705–713; c) S. Goswami, M. K. Gish, J. Wang, R. W. Winkel, J. M. Papanikolas and K. S. Schanze, *ACS Appl. Mater. Interfaces*, **2015**, *7*, 26828–26838; d) T. A. Clem, D. F. J. Kavulak, E. J. Westling and J. M. J. Fréchet, *Chem. Mater.*, **2010**, *22*, 1977–1987; e) C. Y. Liao, C. P. Chen, C. C. Chang, G. W. Hwang, H. H. Chou and C. H. Cheng, *Sol. Energy Mater. Sol. Cells* **2013**, *109*, 111-119.
- S3. M. J. Frisch, G. W. Trucks, H. B. Schlegel, G. E. Scuseria, M. A. Robb, J. R. Cheeseman, G. Scalmani, V. Barone, G. A. Petersson, H. Nakatsuji, X. Li, M. Caricato, A. V. Marenich, J. Bloino, B. G. Janesko, R. Gomperts, B. Mennucci, H. P. Hratchian, J. V. Ortiz, A. F. Izmaylov, J. L. Sonnenberg, D. Williams-Young, F. Ding, F. Lipparini, F. Egidi, J. Goings, B. Peng, A. Petrone, T. Henderson, D. Ranasinghe, V. G. Zakrzewski, J. Gao, N. Rega, G. Zheng, W. Liang, M. Hada, M. Ehara, K. Toyota, R. Fukuda, J. Hasegawa, M. Ishida, T. Nakajima, Y. Honda, O. Kitao, H. Nakai, T. Vreven, K. Throssell, J. A. Montgomery, Jr., J. E. Peralta, F. Ogliaro, M. J. Bearpark, J. J. Heyd, E. N. Brothers, K. N. Kudin, V. N. Staroverov, T. A. Keith, R. Kobayashi, J. Normand, K. Raghavachari, A. P. Rendell, J. C. Burant, S. S. Iyengar, J. Tomasi, M. Cossi, J. M. Millam, M. Klene, C. Adamo, R. Cammi, J. W. Ochterski, R. L. Martin, K. Morokuma, O. Farkas, J. B. Foresman, and D. J. Fox, Gaussian 16, Revision A.03, Gaussian, Inc., Wallingford CT, **2016**.
- S4. a) Q. Zhao, R. G. Parr, *J. Chem. Phys.*, **1993**, *98*, 543-548.; b) C. Lee, W. Yang, R. G. Parr, *Phys. Rev. B*, **1988**, *37*, 785-789.
- S5. T. Lu, F. Chen, *Acta Chim. Sin.*, **2011**, *69*, 2393-2406.
- S6. T. Lu, F. Chen, *J. Comput. Chem.*, **2012**, *33*, 580-592.
- S7. R. D. Dennington, T. A. Keith, J. M. Millam, *GaussView*, 5.0.8; Semichem Inc.:

Shawnee Mission, KS, **2009**.

- S8. M. Sheik-Bahae, A. A. Said, E. W. Van Stryland, *Opt. Lett.*, **1989**, *14*, 955-957.
- S9. M. Sheik-Bahae, A. A. Said, T. H. Wei, D. J. Hagan and E. W. Van Stryland, *IEEE J. Quantum Electron.*, **1990**, *26*, 760-769.
- S10. S. J. Mathews, S. Chaitanya Kumar, L. Giribabu and S. Venugopal Rao, *Optics Communications*, **2007**, *280*, 206-212.